 doi:10.20944/preprints202204.0250.v1

Article

Analysis and Modeling of Soil Salinity Using Sentinel-2A and LANDSAT-8 images in the Afambo Irrigated Area, Afar Region, Ethiopia

Anwar Mohammed [1], Terefe Hanchiso [2, 3, 4*] and Sileshi Abi [1]

[1]College of Dry Land Agriculture, Samara University, P.O. BOX 132, Samara, Ethiopia; anwarmohammed4311@su.edu.et (A.M.)
[2] State Key Laboratory for Subtropical Mountain Ecology of the Ministry of Science and Technology and Fujian Province, Fujian Normal University, Fuzhou 350007, China
[3] Schools of Geographical Sciences, Fujian Normal University, Fuzhou 350007, China
[4] Department of Natural Resource Management, Wolkite University, P.O. Box 07, Wolkite, Ethiopia; sodango27912@alumni.itc.nl
[1]College of Dry Land Agriculture, Samara University, P.O. BOX 132 Samara, Ethiopia, 3; sileshi9@su.edu.et (S.A.)
* Correspondence should be addressed to: anwarmohammed4311@su.edu.et

Abstract: Soil salinity is a severe soil degradation problem mainly faced in arid and semi-arid regions. About 11 million ha of land in the arid, semi-arid, and desert parts of Ethiopia is salt-affected, especially in the Awash River basin, including Afambo irrigated area. Remote sensing approaches are significant tools for accurately predicting and modeling accurately predicting and modeling soil salinity in various world regions. This study aims to analyze and model soil salinity status in the case of Afambo irrigated areas using Landsat-8 and sentinel-2A, Afar region, Ethiopia, by applying remote sensing with field measurements. Thirty-two soil samples were collected from the topsoil (0-30 cm); out of these, 25 soil samples with various EC ranges were selected for modeling, and the remaining 7 samples were utilized to validate the model. Landsat-8 and Sentinel-2A images acquired in the same month were used to extract soil salinity indices. Linear regression analyses correlated the EC data with corresponding soil salinity spectral index values derived from satellite images. The best-performing model was selected for salinity mapping. The soil salinity indices extracted from both Landsat-8 and Sentinel-2A bands estimated soil salinity with high acceptable accuracy of R^2 values of SI, 0.78 and 0.81, respectively. The model results in three salinity classes with varying degree of salinity, namely, highly saline, moderately saline, and slightly saline, which covers 15.1%, 39.8% and 45.1% of the total area for Landsat-8, respectively and 26.1%, 32%, and 41.9% for sentinel 2A, respectively. Generally, the results revealed that the expansion rate of salt-affected soils has been increasing. From this study, it is possible to infer that if the present irrigation practice continues, it is expected that total the cultivated lands will become sterile within a short period. Thus, it needs to be monitored regularly to secure up-to-date knowledge of their extent to improve management practices and take appropriate actions

Keywords: soil salinity; EC; Landsat 8 and Sentinel-2A

1. Introduction

Soil salinization is becoming an increasing downside, particularly in arid and semi-arid regions where irrigation is practiced. Because of salinity and sodicity, soil degradation is increasing at a terrible rate, endangering the surroundings, agricultural ecosystems, and human life [1]. Salinization is one of the most hazardous environmental phenomena that lead to desertification and loss of agricultural productivity [2].

 doi:10.20944/preprints202204.0250.v1

In rain-fed agriculture, water erosion has degraded the soils and depleted the nutrients leading to the increased cost of agriculture production, whereas irrigated agriculture has increased secondary salinization. Therefore, it is imperative to enhance the restoration of degraded agricultural lands to promote sustainable agriculture. The food security gap in African countries can be reduced if land degradation issues are dealt with holistically to conserve soil resources and keep them healthy and fertile[3].

However, the most serious salinity and sodicity problems are faced in irrigated arid and semi-arid regions.

According to [4],Ethiopia is heavily reliant on the agriculture sector for its economic growth and social sector development because it accounts for 40% of the GDP, 80% of the total employment, and 70% of the export earnings. Partial or complete loss of soil productivity attributed to the accumulation of excess salts in the root zone of soils in the arid and semi-arid climates is a worldwide phenomenon.

With the standing of the Ethiopian Irrigation Development Program, 26 medium and large-scale irrigation projects are planned to be implemented. Due to topographic reasons, most of the already established or proposed large-scale irrigation schemes are found in the lowlands of Ethiopia, where major river basins such as Awash, Blue Nile, Wabe Shebelle river basin, and Rift valley lakes basin are located. Over 11 million ha of land in the arid, semi-arid, and desert parts of Ethiopia is known to be salt-affected[5]. The problems of salinity and waterlogging persist in many regions where farmers apply excessive irrigation water, and farmers and irrigation departments fail to invest in adequate drainage solutions[6].

Despite the problems in modeling salinity and relating soil salinity values to radar satellite data, a direct relationship between the Electrical Conductivity (EC) of soils and backscattering images has been proven in some cases. Abdellatif and Mourad, 2017 proposed a parametric formulation to determine salinity from RADARSAT-1 data without a backscattering model. The linear regression analysis was performed, and a good relationship was observed between the measured salinity of the soil samples and the radar images, with a coefficient of determination (R2) of 0.83. Alternatively, soil salinity maps obtained from remotely sensed data, such as satellite scenes or sensors mounted on airplanes, can provide a much faster and more economical way of mapping soil salinity for large areas[7]..

Howari 2007reported that remote sensing has a potential application for rapid and large-scale mapping of salt-affected lands. In recent decades, remote sensing data has been widespread to map soil salinity, either directly from bare soil or indirectly from vegetation, in a real-time and cost-effective manner at various scales[8] . Soil salinity mapping at the regional, national, and farm levels is becoming increasingly important for decision-making and managing soil resources. It is important to generate soil salinity information to determine the extent and further risk of salinity, of which salinity assessment, mapping, and regular monitoring have a great role in salt-affected areas[10].

Despite previous studies in the assessment of soil salinity, studies focusing on the modeling of soil salinity are lacking. Moreover, the previous studies that attempted to map salt-affected soils used low-resolution remote sensing data. However, Sentinel-2A remote sensing products provide high-resolution remote sensing data and may give new emphasis to modeling soil salinity. Therefore, a comprehensive study integrating high-quality remote sensing and GIS approaches is imperative to soil salinity modeling in the semi-arid region, including the Afar region. This study aimed to develop a model that integrates remote sensing with GIS techniques to assess, characterize, and map the state of soil salinity at the Afambo irrigated in the Afar region of Ethiopia.

2. Materials and Methods

2.1. . Description of the Study Area and Sampling Locations

Preprints (www.preprints.org) | NOT PEER-REVIEWED | Posted: 27 April 2022 doi:10.20944/preprints202204.0250.v1

Afambo is one of the Woreda in the Afar Region of Ethiopia. It is part of Administrative Zone one and is bordered on the south by the Somali Region, on the west by Dubti Woreda, on the north by Asayita, and on the east by Djibouti. Geographically, it is bounded by 110 25′0″ N -110 35′0′′ latitude and 410 32′30″-410 40′0″ E longitude. Afambo irrigation farm consists of three Kebeles of the Woreda (Alasabolo, Humedoyta and Mego Kebeles); those Kebeles have covered a total of 11,405 ha.

2.2. Soil sample collection, preparation, and laboratory analysis

A total of 32 soil samples were collected from 3 Kebeles, the soil samples were taken from the topsoil (0-30m) using a hand auger. Purposive random sampling methods were employed. Depending on area of each sampling unit and prevailing micro-variability sufficient number of sub-samples were taken by auger and core sampler were also collected from selected areas. The subsamples were then thoroughly mixed in the field to make one representative composite sample. The coordinates of each sample points were recorded using a portable handheld Global Positioning System (GPS) Garmin version 78

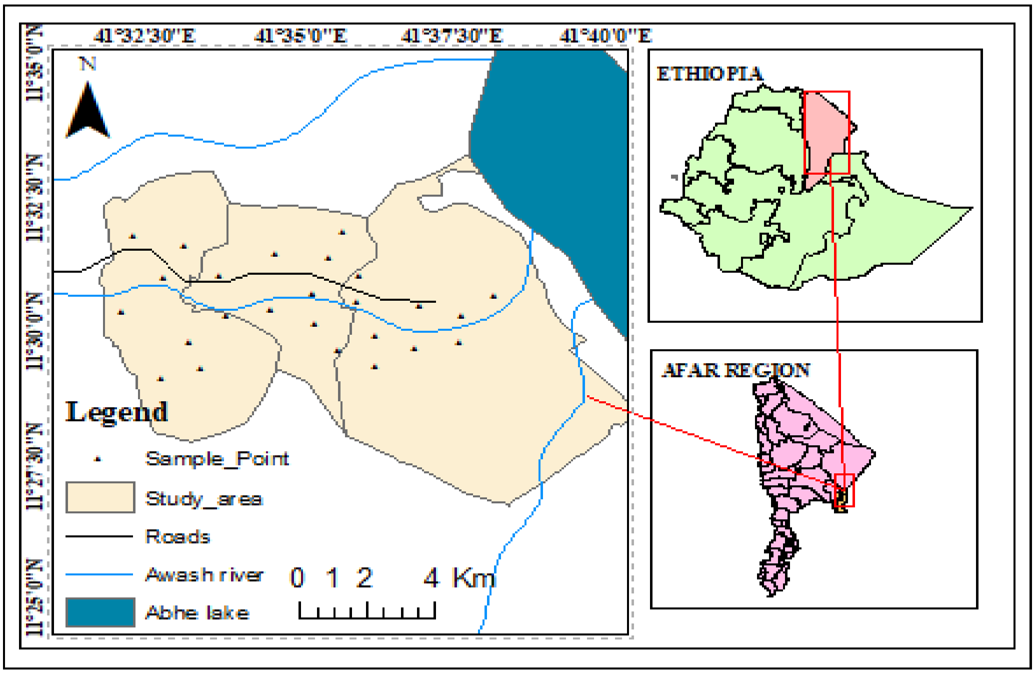

Figure 1. Map of the study area.

Soil samples were air-dried, ground to pass through 2 mm sieve and prepared for the determination of soil salinity indicators. All laboratory analyses were done at laboratories in Dessie soil testing and fertility management center. Electrical conductivity (EC), Soil reaction (pH) soluble cations (Na, Ca, and Mg), exchangeable Na and CEC and, Exchangeable sodium percentage (ESP) were measured. pH and EC were measured in 1:2.5 soils: water suspension using pH meter and conductivity meter, respectively. Exchangeable Ca, Mg and CEC were extracted with 1.0 molar (M) ammonium acetate (NH4OAc) solution. The ammonium displaced from the soil exchange site was distilled and the evolved ammonia was determined by the macro-Kjeldahl method [11] and its concentration was reported as CEC. Exchangeable sodium percentage (ESP) was computed from the data of chemical analysis.

$$ESP = \left(\frac{Na}{CEC}\right)100 \qquad \text{Equation 1}$$

2.3. Image pre-processing

Preprints (www.preprints.org) | NOT PEER-REVIEWED | Posted: 27 April 2022 doi:10.20944/preprints202204.0250.v1

Sentinel-2A provides multispectral data with 13 bands, spanning through visible, near-infrared (NIR), and shortwave infrared (SWIR) with different spatial resolutions ranging from 10 m to 60 m. The Landsat-8 thermal infrared sensor (TIRS) was utilized to evaluate the efficiency of thermal features in soil salinity monitoring. The Sentinel-2A data was downloaded from Sentinel's Scientific Data Hub (https://scihub.copernicus.eu/). The Land sat images were, covering the area of the study site. The Landsat-8 image was downloaded from the United States Geological Survey (USGS) website (www. earth explorer.gov). It should be noted that since optical imagery measures the spectral reflectance of the object's surface, the salinity of the soil surface was assessed in this study. The image was analyzed using ArcGIS 10.7.1, ENVI 4.7, SNAP 64, and SPSS, V23. The Sentinel-2A image was taken Tuesday, February 29, 2021. The OLI image was downloaded from USGS Data Clearinghouse (Earth Explorer). The Sentinel-2A image was corrected and converted to reflectance using the European Space Agency Sentinel Application Platform (SNAP) Sen2Cor module [12]. Two masks were used to exclude the non-soil pixels in both images. The ENVI module "Calculate Cloud Mask using Fmask" was then used to remove any clouds from the images.

2..4. Salinity model development

Soil salinity models were developed using a Land sat-8 image, sentinel-2A, and measured EC data. The model for soil salinity levels mapping from satellite images and EC sampling points was used. The identification of the location of the sampling point on the satellite image was executed. Regression analysis was developed to assess EC's spatial distribution and predict salinity levels at different locations based on EC point data and salinity indices generated from satellite images of (Landsat-8 and sentinel-2A). For this analysis, 25 sample EC points were used based on the result of the soil field. For the regression analysis, the available EC data were acquired in 2020, and the image of 2020 was used to generate salinity and vegetation indices. In this research, multiple linear regression (MLR) techniques; for soil salinity assessment and relating EC values of field samples to salt features were extracted from satellite data. The constructed models were then applied to the entire image to predict EC values for each pixel. The advantage of this model was generalized through GIS because it directly gives the salinity level at any point in the image.

Table 1. The formula used to analyze salinity and vegetation indices for Landsat-8.

Index name	Formula	Reference
SI	$\sqrt{\text{band 3} * \text{band4}}$ or $\frac{\text{Band 3}}{\text{Band 4}}$	[7]
NDSI	$\frac{\text{Band 3} - \text{Band 6}}{\text{Band 6} + \text{Band 3}}$	**[13]**
NDVI	$\frac{\text{Band 5} - \text{Band 4}}{\text{Band 4} + \text{Band 5}}$	**[14]**
SAVI	$\frac{\text{band5} - \text{band4}}{\text{band4} + \text{band5} + L * 1 + L}$ L=0.5	**[14]**
EVI	$\frac{2.5 * (\text{Band5} - \text{Band4})}{\text{Band5} + 6 * \text{Band4} - 7.5 * \text{Band2} + 1}$	[7]

Table 2. The formula used to analyze salinity and vegetation indices for sentinel 2A.

Index name	Formula	Reference
SI	$\frac{\text{Band2} * \text{Band4}}{\text{Band 3}}$	[7]
NDSI	$\frac{\text{Band 3} - \text{Band 11}}{\text{Band 11} + \text{Band 3}}$	[15]
NDVI	$\frac{\text{Band 8} - \text{Band 4}}{\text{Band 4} + \text{Band 8}}$	**[13]**

Preprints (www.preprints.org) | NOT PEER-REVIEWED | Posted: 27 April 2022 doi:10.20944/preprints202204.0250.v1

SAVI	$\frac{band8 - band4}{band4 + band8 + 0.428 * 1.428}$	[14]
EVI	$\frac{2.5 * (Band8 - Band4)}{Band8 + 6 * Band4 - 7.5 * Band2 + 1}$	[15]

2.5. Model comparison and Salinity model performance evaluation

After a map of salt-affected soils were generated from the two models (land sat 8 and sentinel 2) and comparison were made between the two models and finally, the best map was selected. All data are calibrated and validated against the salinity. The root-mean-squared error (RMSE, Eq. (5) is used as metrics to judge the fit of the predicted variables to the observed data when calibrating the parameters of the models [11]

$$RMSE = \frac{1}{n}\sqrt{\sum_{t=1}^{n}(x_m^i - x_o^i)^2} \text{--------------Equation 1}$$

2.6. Model validation and prediction

Validation of the models was done by plotting the EC value with the corresponding raster values of the salinity map generated from satellite imagery for both Landsat-8 and sentinel 2A. Then after linear regression analysis of correlating each salinity index with EC data for both Landsat-8 OLI and Sentinel-2A data was performed to predict the salinity. The main purpose of this process is to increase the statistical reliability of the results.

3. Results and Discussion

2.1. The relationships of EC with Sentinel-2A, and Landsat-8

Remotely sensed data with a significant correlation to EC data for both Landsat-8 OLI and Sentinel-2A data were considered for developing the regression models. The developed regression models are, showing how well spatial variation in soil salinity can be predicted by applying different developed regression models. All the developed regression models were highly significant; for this case, five salinity indices and vegetation index, Soil salinity index (SI), Normalized difference salinity index (NDSI), Normalized difference vegetation index (NDVI), Enhanced vegetation index (EVI), and Soil Adjusted vegetation index (SAVI)) was applied for regression analysis to develop a soil salinity model for both Sentinel-2A and Landsat-8 satellite data [20].

Models were best able to predict soil salinity spatial variation, as they met all the model selection criteria. The soil salinity map with five salty levels serves for land management and agricultural planning.

Remote sensing technology has proven its efficiency in the investigation of soil salinity in a large area. Results show that using Landsat image 8 images and Sentinel-2A images allows one to extract, Mapping, Model, and monitor the features of the salty land. They indicate that the salinity of the Soil has a strong relationship with the reflectance at the NIR channel. This is in line with the results of research presented by [9]. However, the EVI was not highly correlated with EC.

2.2. Regression Models

All five soil salinity indices and vegetation indices (NDVI, NDSI, EVI, SAVI, and SI) were used to conduct multiple regression analyses and linear regression analyses for each satellite data. The resulting models were statistically significant, with the lowest Root mean square error (RMSE) and Mean Absolute error (MAE) except EVI, which is correlated with EC for both Landsat-8 and sentinel- 2A. Linear regression equations of each soil salinity index for Landsat-8and Sentinel-2A data are illustrated in (Figs. 2 and 3), respectively. For generating each soil salinity map, the equations shown in (Figs. 2 and 3) were used to calculate and estimate the corresponding EC value for each pixel. This was done by inserting the salinity index value of each pixel as ‘x’ values in each of the equations. R2

Preprints (www.preprints.org) | NOT PEER-REVIEWED | Posted: 27 April 2022 doi:10.20944/preprints202204.0250.v1

values of linear regression analysis for all indices derived from both satellite data were similar to each other; however, equations obtained from each analysis were different, and, therefore, distinctive soil salinity maps were produced from each index.

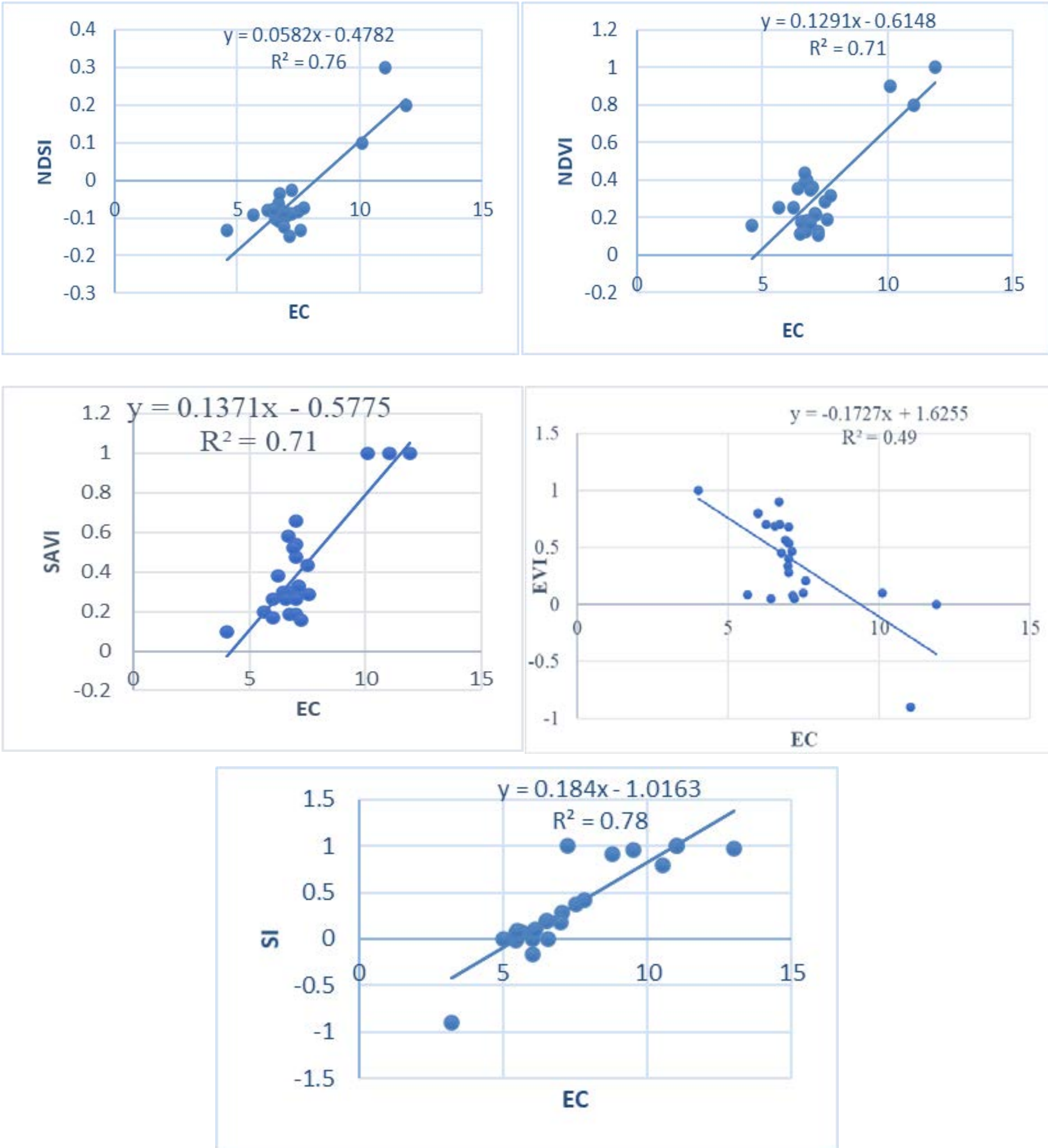

Figure 2. Linear regression results of soil salinity indices derived from Landsat-8 and EC.

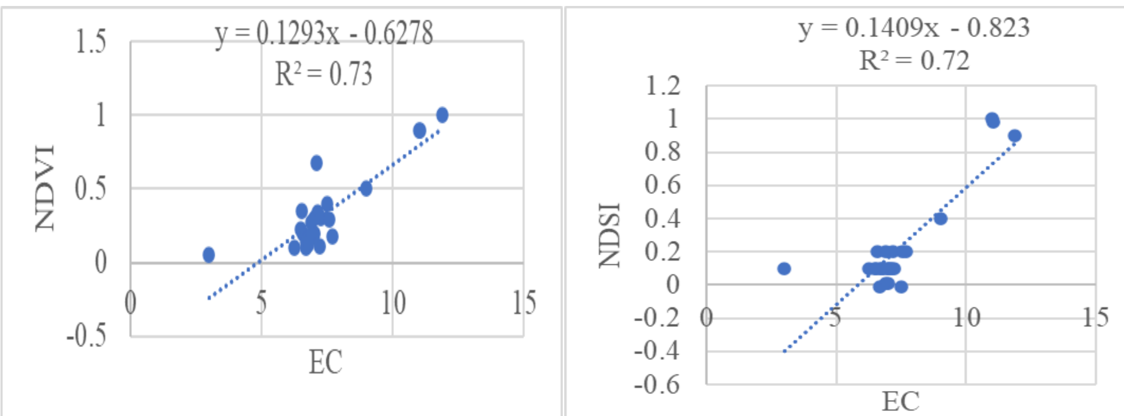

Preprints (www.preprints.org) | NOT PEER-REVIEWED | Posted: 27 April 2022 doi:10.20944/preprints202204.0250.v1

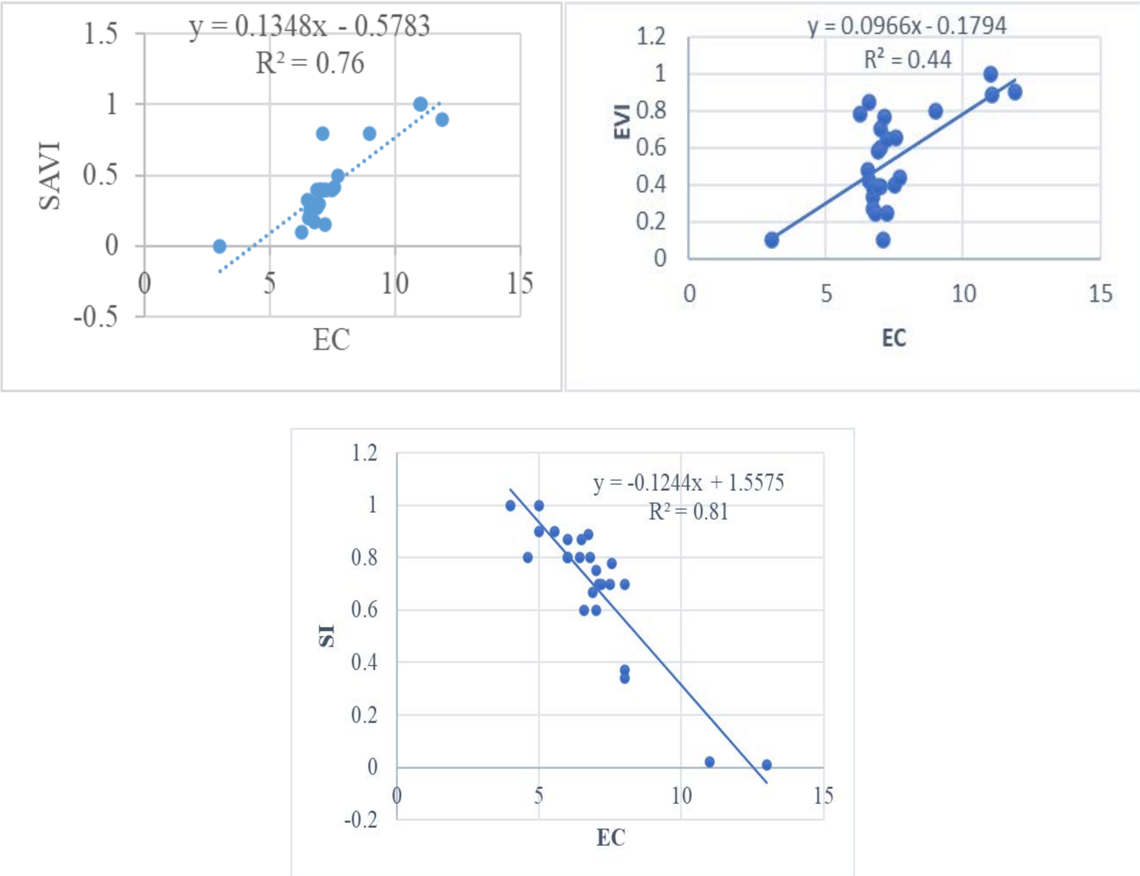

Figure 3. Linear regression results of soil salinity indices derived from sentinel -2A and EC.

According to this graph, it is clear that visible spectral bands, especially the red band, can differentiate the reflectance of each salinity class and, consequently, categorize soil salinity classes. On the other hand, spectral reflectance values of different salinity classes exhibit similar values, making it difficult to differentiate salinity levels for near-infrared and shortwave spectral regions. (Figures 4 and 5) illustrates soil salinity maps generated by applying SI, NDVI, NDSI, and SAVI indices and simple linear regression analysis. There are similarities in all the maps produced using different salinity indexes and satellite data in terms of the spatial distribution of each salinity class.

Preprints (www.preprints.org) | NOT PEER-REVIEWED | Posted: 27 April 2022 doi:10.20944/preprints202204.0250.v1

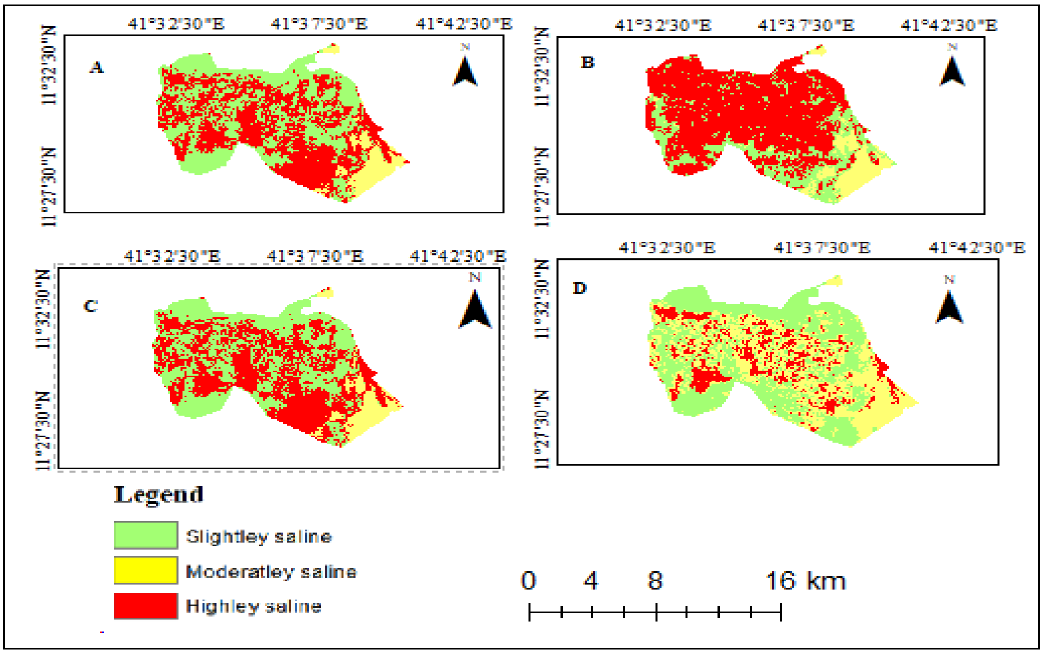

Figure 4. Soil salinity maps of the study area generated from (A)NDVI, (B)NDSI, (C)SAVI, and (D)SI Landsat-8.

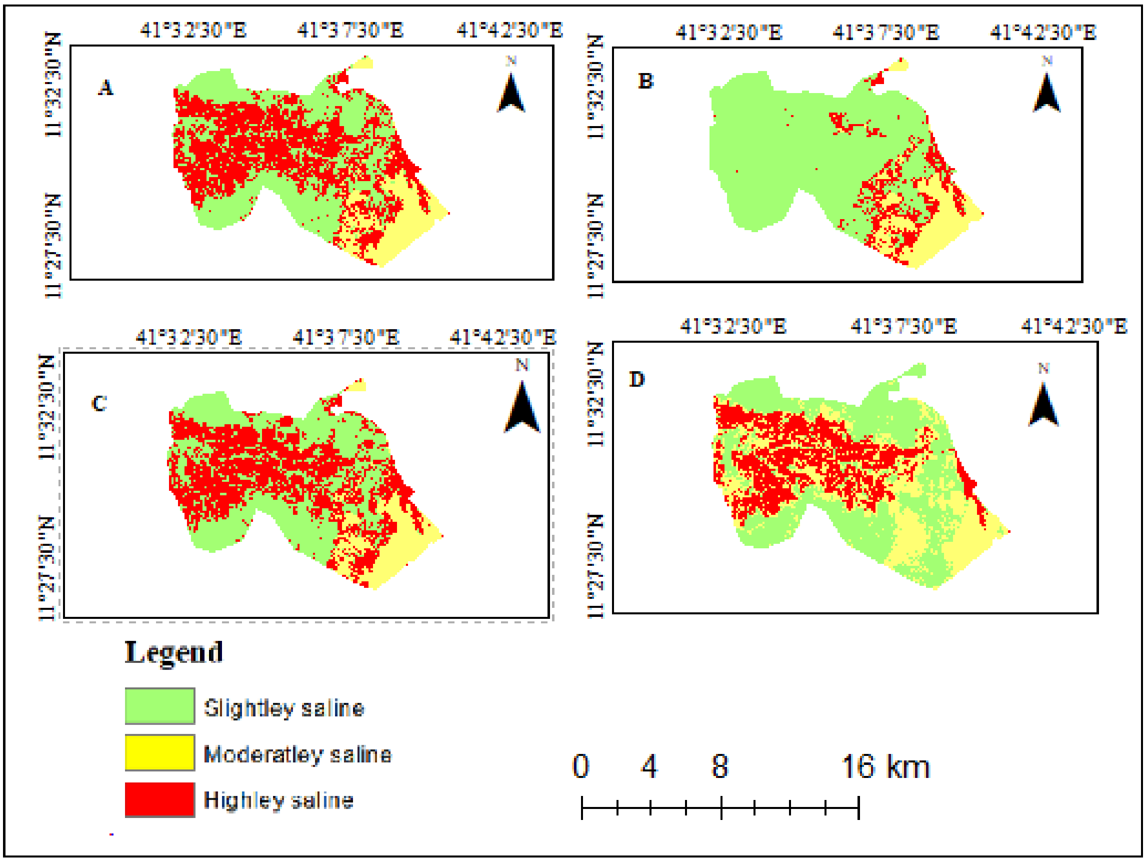

Figure 5. Soil salinity maps of the study area generated from (A) NDVI, (B) NDSI, (C) SAVI, and (D) SI Sentinel-2A.

2.3. *Assessment and Model Validation*

After using the regression method for five indices derived from Landsat data and Sentinel-2A, including NDVI, NDSI, SAVI, EVI, and SI for the soil salinity, it is found that the regression models have a well-defined coefficient (R2) between the salty value obtained from the field measurement and salty values derived from remote sensing data except for EVI. The highest coefficient (R2) from Landsat-8 is 0.78 in the SI model, and from the Sentinel-2A model, the highest coefficient (R2) is 0.81 in the SI model. A similar result is reported by [12] in Tra Vinh Province, where it was affected by salt from the sea due to the tide and rising sea levels. For checking validation of all models, seven similar sample points, including samples from each category of four soil salinity classes, were examined, and the output results for all indices of both satellite data revealed almost similar R2 values ranging from 0.67 to 0. 71..

2.4. *Model comparison*

The models derived from Landsat-8 and Sentinel-2A were compared, and their respective predictions for saline soil of the Afambo irrigated area were produced. Comparing indices generated from Landsat-8, regression result of SI with field data (EC) slightly better R2 value. In addition, the output model of this index exposed a lower Root Mean Square Error (RMSE) of 2.01 and R2 of 0.78. As the same, among indices derived from Sentinel-2A data, the regression result of SI with field data presented (EC) was a slightly better result than the other four indices with R2 and RMSE values of 1.01 and 0.81, respectively. The result suggests that the salinity indices (SI) are the most sensitive to EC in both sensors. The Comparison between the satellite images, Sentinel-2A of SI with field data is a better R2 value and lower mean square error (RMSE) of R2 0.81 and 1.01 respectively than Landsat data. There are similarities in all the maps produced using different salinity indexes and satellite data in terms of the spatial distribution of each salinity class. A comparison of all soil salinity maps generated using indices derived from Sentinel-2A data demonstrated that more land was categorized as slightly saline, particularly in maps produced using NDSI and SI indices. With the same Comparison of all soil salinity maps generated using indices derived from Sentinel-2A data. NDSI categorized more lands as Highly saline. This finding is in agreement with the study [12].

Sentinel-2 is the more useful dataset for identifying salinity change in Afambo irrigated areas. The R2 and RMSE of the models indicate that Sentinel-2 has slightly better skill than Landsat OLI at predicting EC. Sentinel-2A's 10-meter spatial resolution and 2–3-day return time offer a superior spatial and temporal resolution to Landsat-8's 30-meter spatial resolution and 16-day return time.

2.5. *Soil Salinity prediction*

The salinity Prediction model by Landsat-8 and Sentinel-2A for EC vs. SI was prepared using regression analysis. It was observed that the model of EC vs. SI offered a coefficient of determination of 78% and 81% for Landsat-8 and Sentinel-2A, respectively (Fig 6). This model directly gives the salinity level at any point in the image. This prediction model enhances moderately, slightly Saline and highly Saline soil areas. Three ranges of salinity levels were generated from the Landsat-8, and Sentinel-2A predicted salinity map. The summary of salinity level, the extent of the area in hectares and the percentage are given in Table 3.

The model results in three salinity classes with varying degree of salinity, namely, Highly Saline, moderately Saline, and slightly Saline, which covers 15.1%, 39.8% and 45.1% of the total area for Landsat-8, respectively and 26.1%, 32%, and41.9% for sentinel 2A.

Class Name	Salt affected Area (ha)	Percent (%)
Slightly saline	**5149**	**45.1**

Preprints (www.preprints.org) | NOT PEER-REVIEWED | Posted: 27 April 2022 doi:10.20944/preprints202204.0250.v1

Landsat-8	Moderately saline	4534	39.8
	Highly saline	1732	15.1
	Class Name	**Salt affected Area (ha)**	**Percent (%)**
Sentinel 2A	Slightly saline	4780	41.9
	Moderately saline	3648	32
	Highly saline	2987	26.1

Table 1; Soil salinity level derived from prediction model of Landsat-8 and Sentinel 2A

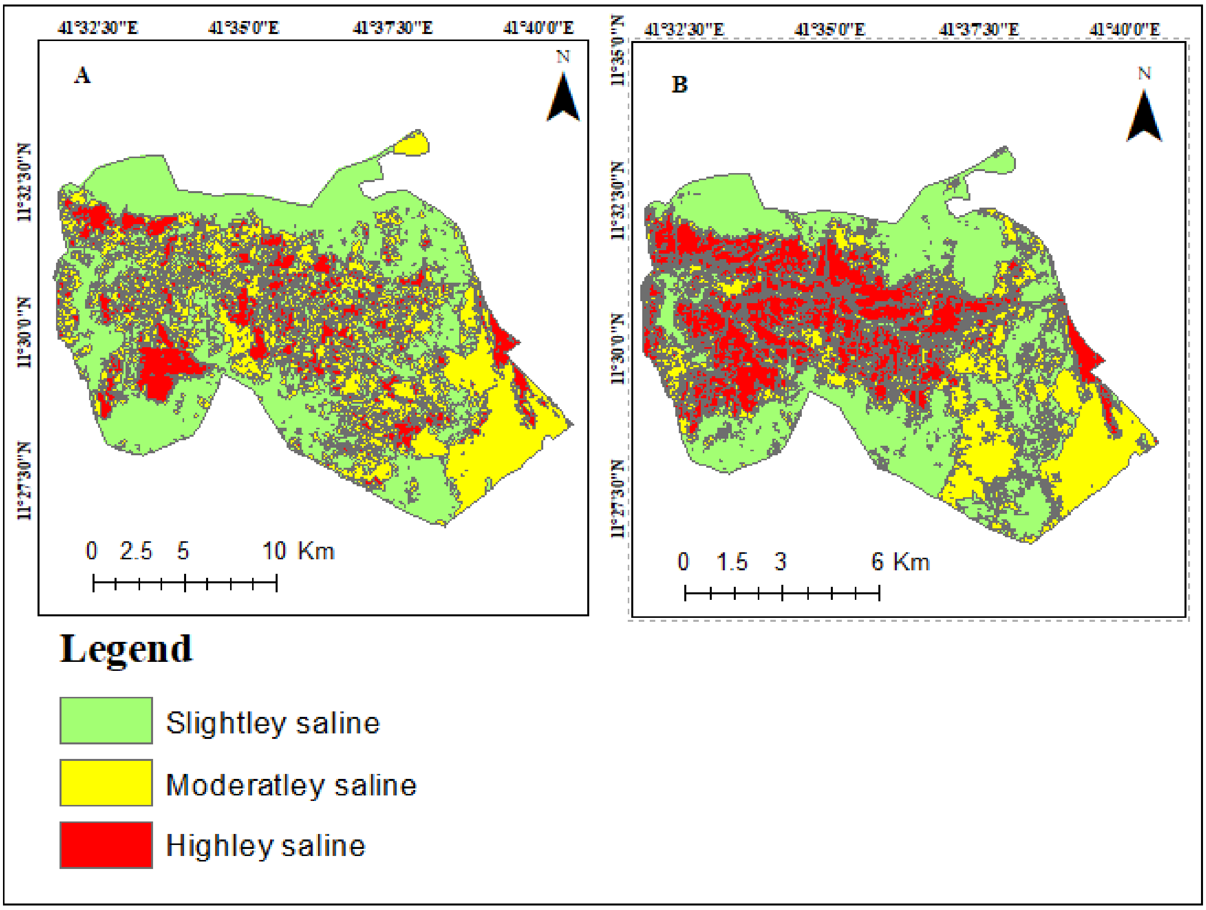

Figure 6. ; Soil salinity maps of the study area using (A) Landsat-8 and (B) Sentinel 2A.

4. Discussion

Remote sensing technology has proven its efficiency in investigating soil salinity in a large area. Results show that using Landsat image 8 images and Sentinel-2A images allows one to extract, Mapping, Model, and monitor the features of the salty land. They indicate that the salinity of the soil has a strong relationship with the reflectance at the NIR channel. The result is in line with the research results presented by [9]. However, the EVI channel does not have a high correlation with EC.

From the regression model, The highest coefficient (R2) from Landsat-8 is 0.78 in the SI model, and from the Sentinel-2A model, the highest coefficient (R2) is 0.81 in the SI model. Similarly, [2] found a strong relationship between the SI and salinity indicator in the red channel, highly correlated with EC. A similar result is reported by [15] in Tra Vinh Province, where it was affected by salt from the sea due to the tide and rising sea levels. All regression models have a high statistical coefficient (R2) with P-value less than 0.05 with acceptable prediction results. Likewise, [16] used an R2 value above 0.66 to get an acceptable and approximate result. This study presented R2 values of 0.78 for Landsat-8 and 0.81 for Sentinel-2A since similar spectral bands of two different satellites were used for a defined window area.

When considering EC measurements showing that salinity impacted land continued beyond the land mapped using the models, the estimate of land affected rises significantly. However, without hyperspectral data, it is not easy to quantify definitively. Based on the results of this study, salinity can be modeled in irrigated land in Afambo. Sentinel-2 and Landsat have similar limitations to their spectral resolution when classifying saline soils though Sentinel-2 has a slightly higher resolution. The higher spatial resolution of Sentinel-2 decreases the number of mixed pixels, likely leading to higher accuracy in classification. Increased spatial resolution and classification accuracy aid in tracking and addressing soil salinization in agricultural fields. As sea levels rise, the land needs to be protected, or practices will need to be adapted to the changes though barriers exist for both options.

5. Conclusion

Soil salinity is one of the major problems affecting agricultural productivity and sometimes becomes too severe to take it out from economic crop production. The demarcation of the location and assessment of the extent and severity of soil salinity is a prerequisite for any reclamation process. This research deals with the modeling of salt-affected soils with the help of remote sensing technologies in the Afambo irrigated area. Satellite data has offered cost-effective and rapid temporal monitoring and detection of soil salinity on a field to regional scale over the last three decades. In recent years, multi-spectral sensors such as Landsat-8 and Sentinel-2A have been used to quantify soil salinity in various case studies. The capacity and utility of Landsat-8 and Sentinel-2A for soil salinity modeling were examined in this work. Two regression models and five soil salinity indices and vegetation indices were used. Soil salinity Prediction models were developed to Model salt-affected areas, derived from the correlation of measured EC value and salinity index (SI) derived from Landsat image and Sentinel 2A. The combination of these remotely sensed variables into one model explained with R2 78% for Landsat-8 and R2 81% for Sentinel-2A of the spatial variation of salinity in the area. Finally, It is important to note that different satellite images and salinity indices may be applied and discussed in similar other studies, and the need for further and future investigation of such dependencies may be required. In order to assess the reliability of the method applied, it is recommended to execute similar studies in the rift valley having similar agro-ecological conditions. Soil salinity processes are highly dynamic. Therefore, the method of detecting soil salinity should also be dynamic.

Author Contributions: Conceptualization, A.M., T.H.S; Methodology, A.M., T.H.S.; software, A.M., T.H.S.; Validation, A.M., T.H.S.; formal analysis, A.M., T.H.S.; Investigation, A.M., T.H.S.; resources, A.M., T.H.S., data curation, A.M.; writing-original draft preparation; A.M.; writing-review and editing, T.H.S.; supervision, T.H.S., S.A. All authors read and approved the final manuscript.

Funding: This study was supported by Ministry of Education, Democratic Republic of Ethiopia.

Institutional Review Board Statement: Not applicable.

Informed Consent Statement: Not applicable.

Data Availability Statement: The data presented in this study are available on request from the corresponding author.

Conflicts of Interest: The authors declare no conflicts of interest.

Reference

1. Shegena, Z., K.V. Suryabhagavan, and M. Balakrishnan, Geo-spatial approach for soil salinity mapping in Sego Irrigation Farm, South Ethiopia. Journal of the Saudi Society of Agricultural Sciences, 2017. 16(1): p. 16-24.
2. Amal, A., K. Lalit, and S. Priyakant, Mapping and Modelling Spatial Variation in Soil Salinity in the Al Hassa

Preprints (www.preprints.org) | NOT PEER-REVIEWED | Posted: 27 April 2022 doi:10.20944/preprints202204.0250.v1

Oasis Based on Remote Sensing Indicators and Regression Techniques. Remote sensing (Basel, Switzerland), 2014. 6(2): p. 1137-1157.
3. Siddiqui, M.S. and D.W. Fowler, Effect of Internal Water Pressure on the Measured Coefficient of Thermal Expansion of Concrete. Journal of materials in civil engineering, 2015. 27(4): p. 4014151.
4. AFRICAN DEVELOPMENT BANK-ARAB BANK FOR ECONOMIC DEVELOPMENT IN AFRICA-ASIAN DEVELOPMENT BANK-CARIBBEAN DEVELOPMENT BANK-INTER-AMERICAN DEVELOPMENT BANK-WORLD BANK-COMMISSION OF EUROPEAN COMMUNITIES-ORGANIZATION OF AMERICAN STATES-UNITED NATIONS DEVELOPMENT PROGRAM-UNITED NATIONS ENVIRONMENT PROGRAM: DECLARATION OF ENVIRONMENTAL POLICIES AND PROCEDURES RELATING TO ECONOMIC DEVELOPMENT. International legal materials, 1980. 19(2): p. 524-525.
5. Dinka, M.O., W. Loiskandl, and J.M. Ndambuki, Hydrologic modelling for Lake Basaka: development and application of a conceptual water budget model. Environ Monit Assess, 2014. 186(9): p. 5363-5379.
6. Wichelns, D. and M. Qadir, Achieving sustainable irrigation requires effective management of salts, soil salinity, and shallow groundwater. Agricultural water management, 2015. 157: p. 31-38.
7. Abdellatif, D. and L. Mourad, Optical tool for salinity detection by remote sensing spectroscopy: application on Oran watershed, Algeria. J. Appl. Remote Sens, 2017. 11(3): p. 036010-036010.
8. Howari, F.M., The use of remote sensing data to extract information from agricultural land with emphasis on soil salinity. Australian journal of soil research, 2003. 41(7): p. 1243-1253.
9. Metternicht, G., et al., Remote Sensing of Soil Salinization. 2009, Baton Rouge: CRC Press.
10. Shahid, S.A., M.A. Abdelfattah, and F.K. Taha, Developments in Soil Salinity Assessment and Reclamation Innovative Thinking and Use of Marginal Soil and Water Resources in Irrigated Agriculture. 1st 2013. ed, ed. C. International Conference on Soil and E. Reclamation of Degraded Lands in Arid. 2013, Dordrecht: Springer Netherlands : Imprint: Springer.
11. Jackson, T.M., et al., Building a climate resilient farm: A risk based approach for understanding water, energy and emissions in irrigated agriculture. Agricultural systems, 2011. 104(9): p. 729-745.
12. Xingwang, F., et al., Soil Salinity Retrieval from Advanced Multi-Spectral Sensor with Partial Least Square Regression. Remote sensing (Basel, Switzerland), 2015. 7(1): p. 488-511.
13. Khan, N.M., et al. Agricultural water management. Amsterdam: Elsevier Science.
14. Alhammadi, M.S. and E.P. Glenn, Detecting date palm trees health and vegetation greenness change on the eastern coast of the United Arab Emirates using SAVI. International journal of remote sensing, 2008. 29(6): p. 1745-1765.
15. https://www.bluemarblegeo.com/knowledgebase/global-mapper-19/Raster_Calculator.htm.
16. Farifteh, J., A. Farshad, and R.J. George, Assessing salt-affected soils using remote sensing, solute modelling, and geophysics. Geoderma, 2006. 130(3-4): p. 191-206.